Blue-Green Systems

IWA PUBLISHING

Blue-Green Systems Vol 2 No 1
doi: 10.2166/bgs.2020.914

Water quality performance of a permeable pavement and stormwater harvesting treatment train stormwater control measure

Ryan J. Winston[a,*], Kristi Arend[b], Jay D. Dorsey[c] and William F. Hunt[d]

[a] Departments of Food, Agricultural and Biological Engineering and Civil, Environmental, and Geodetic Engineering, Ohio State University, 590 Woody Hayes Drive, Room 230, Columbus, OH 43210, USA

[b] Ohio Department of Natural Resources, Old Woman Creek National Estuarine Research Reserve, 2514 Cleveland Road East, Huron, OH 44839, USA

[c] Research Scientist, Department of Food, Agricultural and Biological Engineering, Ohio State University, 590 Woody Hayes Drive, Columbus, OH 43210, USA

[d] William Neal Reynolds Distinguished Professor and Extension Specialist, Department of Biological and Agricultural Engineering, North Carolina State University, Box 7625, Raleigh, NC 27695, USA

*Corresponding author. E-mail: winston.201@osu.edu

Abstract

Stormwater runoff from urban development causes undesired impacts to surface waters, including discharge of pollutants, erosion, and loss of habitat. A treatment train consisting of permeable interlocking concrete pavement and underground stormwater harvesting was monitored to quantify water quality improvements. The permeable pavement provided primary treatment and the cistern contributed to final polishing of total suspended solids (TSS) and turbidity concentrations (>96%) and loads (99.5% for TSS). Because of this, >40% reduction of sediment-bound nutrient forms and total nitrogen was observed. Nitrate reduction (>70%) appeared to be related to an anaerobic zone in water stored in the scarified soil beneath the permeable pavement, allowing denitrification to occur. Sequestration of copper, lead, and zinc occurred during the first 5 months of monitoring, with leaching observed during the second half of the monitoring period. This was potentially caused by a decrease in pH within the cistern or residual chloride from deicing salt causing de-sorption of metals from accumulated sediment. Pollutant loading followed the same trends as pollutant concentrations, with load reduction improved vis-à-vis concentrations because of the 27% runoff reduction provided by the treatment train. This study has shown that permeable pavement can serve as an effective pretreatment for stormwater harvesting schemes.

Key words: green infrastructure, pervious pavement, porous pavement, rainwater harvesting, series, WSUD

INTRODUCTION

Urbanization results in the construction of impervious surfaces, increasing the rate and volume of stormwater runoff. These changes in land use cause negative impacts to streams and surface waters (Walsh *et al.* 2005), including an increase in nutrient, sediment, bacterial, heavy metal, and chloride loads, all of which pose threats to surface water quality (Bannerman *et al.* 1993; Davis *et al.* 2001).

Blue-Green Systems Vol 2 No 1
doi: 10.2166/bgs.2020.914

To mitigate some of these negative consequences, stormwater control measures (SCMs) are employed. Two common green infrastructure SCMs are permeable pavement, which allows water to infiltrate rather than run off the pavement, and rainwater harvesting, which provides a source of water for various uses (Brattebo & Booth 2003; Gee & Hunt 2016). There is burgeoning evidence in the literature that placing SCMs in series using a 'treatment train' approach can provide synergistic benefits (Hathaway & Hunt 2009; Doan & Davis 2017).

Permeable pavement consists of a porous surface course with layers of open-graded aggregate beneath which provide structural support and void space for stormwater infiltration and subsequent storage. Permeable pavements sequester sediment and heavy metals effectively through filtration at the surface course and sedimentation within the storage reservoir (Roseen *et al.* 2012; Drake *et al.* 2014a). Extending detention within permeable pavements using an internal water storage (IWS) zone or throttling the underdrain flow using a valve may increase runoff reduction through exfiltration and create conditions ripe for denitrification (Wardynski *et al.* 2012; Braswell *et al.* 2018). If properly designed and maintained, permeable pavements could provide a first level of water quality treatment within a stormwater harvesting scheme. Typical maintenance regimes involve the removal of the upper 25 mm of accumulated detritus, providing (1) for the hydraulic function of the pavement and (2) removing accumulated sediment-bound pollutants, such as heavy metals, from the SCM (Legret & Colandini1999; Winston *et al.* 2016a).

Rainwater harvesting SCMs capture runoff in a tank for storage and use during dry periods. DeBusk & Hunt (2014) observed significant reductions in both N and P species within rainwater harvesting systems; others have also found water quality improvements due to settling and chemical processes within the tanks (Despins *et al.* 2009; Sung *et al.* 2010). Given the desire to reduce potable water use and associated costs, harvesting stormwater by using permeable pavement as a pretreatment to an underground cistern could be a useful treatment train approach. Until recently, this type of stormwater harvesting for non-potable uses has not been considered a viable option, because parking lot runoff was viewed as 'too dirty' for beneficial use. Gomez-Ullate *et al.* (2011) presented the idea of using permeable pavement exfiltrate as a resource for non-potable water supply. However, no field research studies have yet been carried out on the performance of these two SCMs in series. As such, the aims of this study were threefold: (1) quantify improvement in pollutant concentrations, (2) quantify reduction in pollutant loads, and (3) understand the pollutant removal mechanisms at play in a permeable pavement and stormwater harvesting treatment train.

MATERIALS AND METHODS

Site description

A permeable interlocking concrete pavement (PICP) retrofit underlain by a cistern made up of two interconnected concrete vaults was constructed in June through July 2014 at the Old Woman Creek National Estuarine Research Reserve visitor center parking lot located in Huron, Ohio (Figure 1). The SCM was constructed on poorly draining hydrologic soil group (HSG) D soils (Del Ray silty clay soil; Soil Survey Staff 2015), with average infiltration rates of 0.046 mm/hr measured in soil pits located within the permeable pavement extent (Winston *et al.* 2020).

Pretreatment for the cistern was provided by 270 m^2 of PICP retrofitted in the parking stalls of an existing parking lot (Figures 1 and 2). Run-on from 465 m^2 of adjacent impervious asphalt drained onto the PICP. Because the cisterns were located beneath the PICP, they eliminated exfiltration (i.e., infiltration into the underlying soil) from a portion of the PICP subgrade, reducing the effective exfiltrative surface area to 246 m^2. The run-on ratio (1.7:1), which can be used as a measure of clogging, was defined as the ratio of the contributing watershed area to the permeable pavement surface

Blue-Green Systems Vol 2 No 1
doi: 10.2166/bgs.2020.914

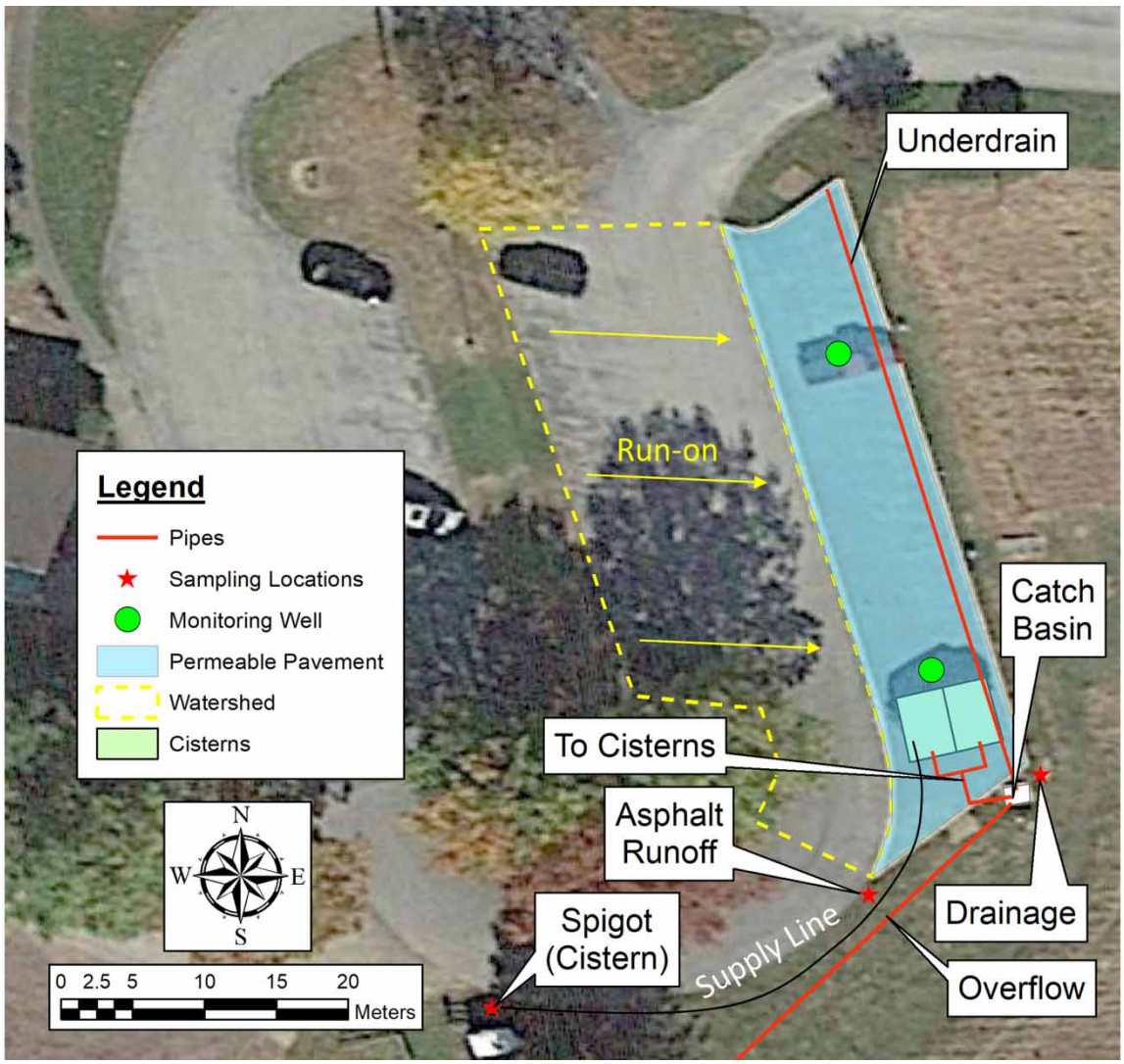

Figure 1 | Plan view of the treatment train showing the permeable pavement and its contributing drainage area, underground cistern, and pipe network. Sampling locations are shown with red stars.

area. The hydrologic loading ratio (1.9:1), which is a surrogate for hydrologic performance, was defined as the ratio of the contributing watershed area to effective exfiltrative surface area.

From the bottom of the cross-section, the aggregate layers supporting the PICP included 46–56 cm of American Association of State Highway and Transportation Officials (AASHTO) #4 aggregate (19–37 mm nominal diameter), 10 cm of AASHTO #57 aggregate (2.4–37 mm nominal diameter), and 5 cm of AASHTO #89 aggregate (1.2–12.5 mm nominal diameter; Figure 2). Aggregate was placed in 15-cm lifts and compacted with a 10-ton roller. The PICP was installed on the bedding course of AASHTO #89 aggregate. A 15-cm diameter perforated PVC underdrain was installed 7.5 cm above the bottom of the cross-section, creating an IWS zone (Figure 2). The underdrain was routed to a catch basin adjacent to the permeable pavement, where stormwater was conveyed to the cistern until it filled, at which point the hydraulic gradient caused overflow (Figure 1).

The cistern was made up of two interconnected concrete vaults, which were each 90-cm tall, 244-cm wide, and 488-cm long, and were hydraulically connected with three booted 15-cm PVC pipes resulting in a total of 11,900 L of storage volume (Figure 2). They were fitted with concrete tops and eccentric cone manways to allow maintenance access from the surface. The cisterns were covered with 45 cm of clay soil compacted to 95% Proctor compaction. The PICP base and subbase

Blue-Green Systems Vol 2 No 1
doi: 10.2166/bgs.2020.914

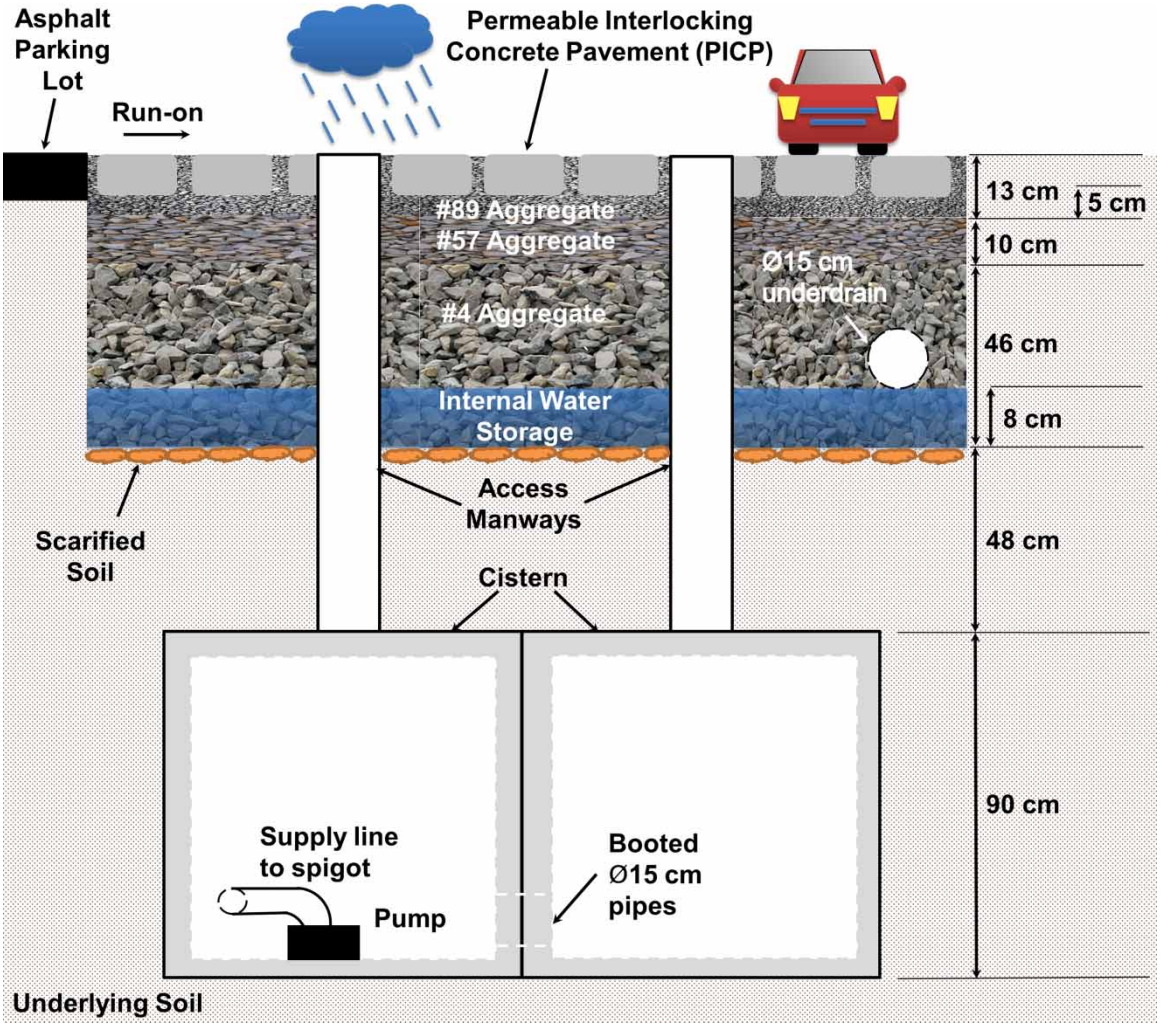

Figure 2 | Cross-sectional view of permeable pavement and cistern treatment train. Note that the cistern was only located under approximately 10% of the permeable pavement surface area (see Figure 1).

aggregate courses extended across the top of this compacted clay (Figures 1 and 2). The cistern was designed to receive drainage from the permeable pavement underdrains; once filled, drainage from the PICP was designed to overflow to Old Woman Creek through a 20-cm diameter PVC pipe. An on-demand submersible pump with a floating intake was installed in one of the concrete vaults to convey harvested stormwater through a supply line to a nearby spigot, where it could be used for landscape irrigation and vehicle washing.

Data collection

Rainfall data were collected on-site using a 0.25-mm resolution Davis Rain Collector tipping bucket rain gauge (Davis Instruments, Hayward, CA) attached to a 2-m tall wooden post in a location free from overhead obstructions. The rainfall depth over each 1-minute interval was recorded on a data-logger. When these data were deemed unreliable, 15-minute interval rainfall data from an on-site National Oceanic and Atmospheric Administration (NOAA)-maintained rain gauge were utilized. An on-site manual rain gauge (Productive Alternatives, Fergus Falls, MI) was used to determine event rainfall depth.

Hobo U20 pressure transducers (Onset Computer Corporation, Bourne, MA), ISCO 730 bubbler flow meters (Teledyne ISCO, Lincoln, NE), and strategically placed weirs were utilized to determine

Blue-Green Systems Vol 2 No 1
doi: 10.2166/bgs.2020.914

the water balance in the treatment train (see Winston *et al.* 2020, for additional details). Two shallow monitoring wells were installed during construction within the open-graded aggregate reservoir beneath the PICP (Figure 1), and Hobo U20 pressure transducers measured water level in each well. Inflow to (i.e., drainage from the PICP) and withdrawals from the cistern for irrigation and car washing were measured by placing a HOBO U20 pressure transducer at the bottom of the cistern. When the cistern was full, overflow to Old Woman Creek estuary occurred; this was measured using a 60° v-notch weir and a Hobo U20 pressure transducer in a weir box. All Hobo and ISCO flow data were collected on a 2-minute interval and stored on internal memory. A U20 pressure transducer was utilized to measure (and subsequently correct for) variations in on-site barometric pressure.

Water quality samples were obtained from three locations in the treatment train: a control, impervious asphalt location (representative of the run-on to the permeable pavement; hereafter 'asphalt'), from the underdrain of the permeable pavement (hereafter 'drainage'), and from the spigot (hereafter 'cistern') which represented the point-of-use water quality (Figure 1). The asphalt location consisted of a 2-ft wide sample collection trough installed at the parking lot edge to capture runoff from a representative impervious catchment adjacent to the PICP. A small notch in the flush curb directed flow into the sampling trough. Samples of asphalt runoff were triggered based on rainfall depth, which, following minor rainfall abstraction in an asphalt parking lot, is a direct indicator of runoff volume. An ISCO 6712 sampler was utilized to obtain 200-mL aliquots from the sampling trough after each 0.05 inches of rainfall, thus obtaining runoff volume-proportional, composite samples (Teledyne ISCO, Lincoln, NE).

Runoff volume-proportional, composite samples were also collected using an ISCO 6712 sampler at the drainage (i.e. flow from the PICP underdrain) monitoring location to isolate treatment by the permeable pavement. The underdrain was throttled through several orifices designed to control dewatering of the storage reservoir, including 19 mm, 50 mm, and 100 mm orifices set at 0 mm, 165 mm, and 420 mm above the drain invert. After flow was throttled, it discharged into a weir box, where an ISCO 730 bubbler module (Teledyne ISCO, Lincoln, NE) measured flow depth over a 30° v-notch weir. Measured flow depth was converted to flow rate using standard weir equations. Flow rate was integrated with time to determine stormwater volume and trigger sample aliquots; aliquots at a given monitoring point were composited, characterizing pollutant event mean concentrations (EMC) over the hydrograph.

To determine stormwater quality after treatment by the permeable pavement and cistern, water quality samples were obtained from the spigot, which utilized an on-demand, submersible pump (Amphibian J125, 11/4 HP pump; Conservation Technology, Baltimore, MA) to draw water from the cistern. The pump employed a floating intake but lacked UV or grit filtration. The spigot was allowed to flow for 30 seconds before a grab sample of stormwater stored in the cistern was obtained. Water quality samples were obtained from the spigot 7.8 $\pm$ 5.7 hours (mean $\pm$ standard deviation) after rainfall ended.

All composite samples were composed of a minimum of five aliquots and described greater than 80% of the pollutograph. All samples were collected within 18 hours of the cessation of rainfall. Samples were obtained from locations where flow was well mixed and sample intake strainers were used to remove gross solids.

Laboratory methods

Composite samples from the asphalt and drainage sampling locations were shaken vigorously in the 10-L composite bottles to re-suspend solids, and were then subsampled into laboratory containers. Composite samples were divided among two 1-L plastic bottles for TSS analysis, one 500-mL pre-acidified bottle for nutrient analysis, one 500-mL pre-acidified bottle for metals analysis, and a 50-mL glass jar (following field filtration through a Whatman Puradisc 0.45-μm filter) for orthophosphate (OP)

Blue-Green Systems Vol 2 No 1
doi: 10.2166/bgs.2020.914

analysis. Spigot grab samples were dispensed into each sample bottle separately. Samples were placed immediately on ice and chilled to less than 4 °C for transit to the laboratories. Samples destined for the Northeast Ohio Regional Sewer District Laboratory [total Kjeldahl nitrogen (TKN), and the metals aluminum (Al), calcium (Ca), copper (Cu), iron (Fe), magnesium (Mg), manganese (Mn), sodium (Na), lead (Pb), and zinc (Zn)] were shipped overnight on ice. The following pollutants were analyzed at the on-site water quality laboratory at Old Woman Creek National Estuarine Research Reserve: nitrate (NO_3), nitrite (NO_2), ammonia (NH_3), OP, total phosphorus (TP), total suspended solids (TSS), chloride (Cl), silicate, and sulfate. Turbidity, pH, and total alkalinity were also measured. Total nitrogen ($TN = TKN + NO_{2\text{-}3}$), organic nitrogen ($ON = TKN - TAN$), and particle-bound phosphorus ($PBP = TP - OP$) concentrations were calculated. Samples were analyzed using either USEPA (1983) or American Public Health Association (APHA *et al.* 2012) methods.

Data analysis

Separate storm events were characterized by a minimum antecedent dry period (ADP) of 6 hours and rainfall depth of 2.5 mm. Summary statistics for each precipitation event were developed, including rainfall depth (mm), rainfall duration (hrs), average rainfall intensity (mm/hr), peak rainfall intensity (maximum over any 5-minute duration, mm/hr), and ADP (days).

Measurement of run-on to the permeable pavement was not possible since diffuse inflow occurred along its upslope end (Figure 1). Runoff entering the permeable pavement from the 100% impervious catchment was determined for each qualifying rainfall event using a rainfall-runoff model, the NRCS curve number method (Winston *et al.* 2020). To determine the drainage and overflow rates, standard equations for 30° and 60° v-notch weirs, respectively, were used to determine flow rate from measured flow depth. Hydrographs were integrated with time to determine drainage and overflow volumes for use in pollutant load determination. The cistern water level as a function of time was compared to the overflow pipe invert elevation to corroborate periods of overflow. Similarly, the monitoring well water levels were used to corroborate periods of drainage.

The performance of the treatment train for metals, sediment, chloride, nutrients, pH, alkalinity, silicate, and sulfate was determined by comparing EMCs from the asphalt, drainage, and cistern monitoring points. Summary statistics were developed for EMCs from each monitoring location, including the range, mean ($\bar{x}$), median ($\tilde{x}$), standard deviation (s), coefficient of variation (CV), efficiency ratio (ER), and median relative efficiency (RE_{median}). The latter three statistics are defined below:

$$CV = \frac{s}{\bar{x}} \tag{1}$$

$$ER = 1 - \frac{\sum_{i=1}^{n} (EMC_{EFF,i})/n}{\sum_{i=1}^{n} (EMC_{INF,i})/n} \tag{2}$$

$$RE_{median} = 1 - \frac{EMC_{EFF,med}}{EMC_{INF,med}} \tag{3}$$

where n is the number of sampled storm events, EMC_{EFF} is the effluent EMC, EMC_{INF} is the influent EMC, and EMC_{med} is the median EMC at a particular monitoring location. Since only two drainage events were sampled, ER and RE_{median} were determined between the asphalt and cistern monitoring points only. Evaluating the ER and RE_{median} statistics without regard for influent concentration can lead to misleading conclusions, since they are heavily influenced by low or irreducible influent concentrations (Strecker *et al.* 2001). Boxplots were created for each pollutant to examine differences in water quality. Since only two drainage samples were obtained, drainage concentrations were plotted as symbols over the cistern sample boxplots.

Blue-Green Systems Vol 2 No 1
doi: 10.2166/bgs.2020.914

A value of one-half the detection limit was substituted for pollutant concentrations below the method detection limit (MDL). The only analytes which exhibited frequent (i.e., greater than half of the 16 sampled events) below detection limit (BDL) concentrations were chloride ($n = 10$ for asphalt) and nitrite ($n = 10$ for asphalt and cistern). Orthophosphate ($n = 6$ and 8 storms) and TSS ($n = 0$ and 8 storms) concentrations were BDL for a moderate number of events for asphalt and cistern monitoring locations, respectively. For all other analytes, BDL concentrations were observed for fewer than 10% of sampled storm events. All concentrations above MDL were analyzed without alteration.

Influent and effluent pollutant loads for the treatment train were determined as the product of EMC and volume for each storm event. Storms that did not produce overflow were assumed to contribute no effluent pollutant load to Old Woman Creek. Effluent loading was determined as the product of the cistern concentration and the overflow volume, since overflow only occurred when the cistern was full. Sampled storm influent and effluent loads were tabulated for comparison. A summation of load (SOL) was then determined for each pollutant:

$$SOL = \left(1 - \frac{\sum_{i=1}^{j} L_{Out,i}}{\sum_{i=1}^{j} L_{in,i}}\right) \times 100 \tag{4}$$

where j is the number of sampled storm events for a particular pollutant and L is the pollutant load (kg) for the i^{th} event. Annual loading was determined by accounting for non-sampled storms. For these events, the product of the median EMC and the total non-sampled storm volume was added to the sampled storm load. The resulting load was then normalized by watershed area (A, ha), and monitoring period duration (d_{MP}, years), resulting in an annual loading (kg/ha/yr):

$$L_a = \frac{\sum_{i=1}^{j} (EMC_{o,i} \times V_{l,i}) + \sum_{k=1}^{l} (V_{o,k}) \times EMC_{med}}{A \times d_{MP}} \tag{5}$$

where l is the number of non-sampled storms for a particular pollutant, o is the monitoring location of interest, V is stormwater volume, and EMC_{med} is the median observed EMC for sampled events. Pollutant loading for drainage samples was not determined due to the small sample size ($n = 2$).

All data analysis was completed using R statistical software version 3.3.2 (R Core Team 2017). Paired comparisons of pollutant concentration and pollutant load were made to determine statistical significance between monitoring locations. If data were normal or log-normal, a paired t-test was utilized; otherwise, a Wilcoxon rank sum test was applied without transformation of the data. Square root transformation was applied to chloride, since some of the reported concentrations were zero. Normality was assessed through analysis of quantile-quantile plots and using five normality tests (Anderson-Darling, Cramer Von-Mises, Pearson Chi-Square, Shapiro-Francia, and Shapiro-Wilk). Statistical analyses related to water quality compared the asphalt and cistern monitoring locations only due to the small drainage data set ($n = 2$). Statistical testing was performed using a criterion of 95% confidence ($\alpha = 0.05$) unless otherwise noted.

RESULTS AND DISCUSSION

Observed rainfall events and runoff hydrology

Seventy-two separate precipitation events were observed during the 13-month period from August 2014–2015 (Figure 3). Of these, 13 snow or mixed precipitation events were removed from the analysis because they resulted in unreliable hydrologic data. Of the remaining 59 events, paired water quality samples were obtained from the asphalt and cistern monitoring sites for 16 events. Storm

Blue-Green Systems Vol 2 No 1
doi: 10.2166/bgs.2020.914

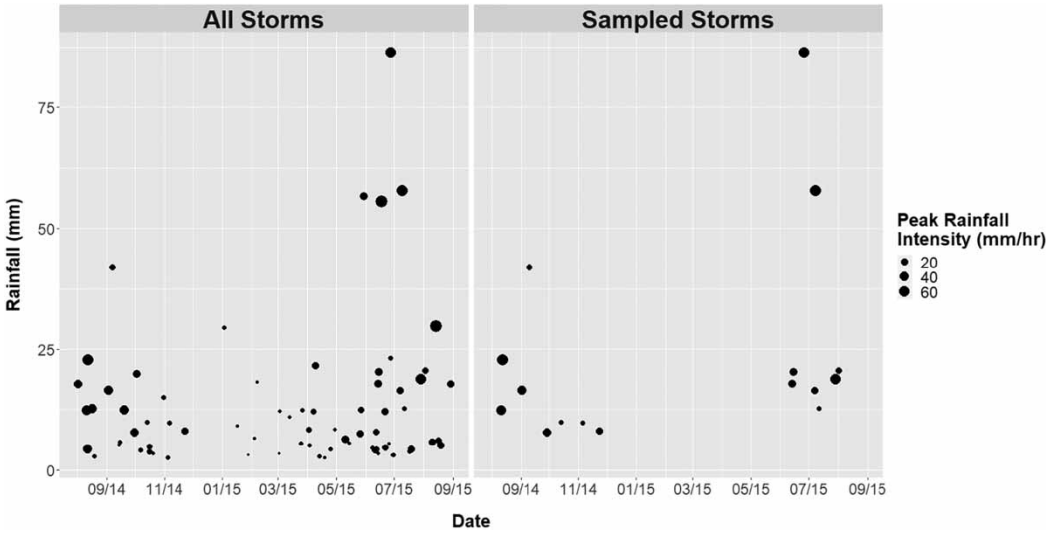

Figure 3 | Rainfall depth and peak rainfall intensity for all observed storms and storms sampled for water quality.

events sampled for water quality represented 380 mm, or approximately 40%, of the 1,098 mm of precipitation that occurred during the monitoring period. Median sampled storm event depth was 17.3 mm, while the median overall storm depth was 8.4 mm. Median peak rainfall intensity for sampled storms was higher than for all observed storms (28.7 mm/hr vs. 11.2 mm/hr). Median antecedent dry period for sampled events (5.6 days) was also larger than for all observed storms (3.5 days). These data suggest that sampled storms were larger and more intense than the central tendency, mainly due to the difficulty in successfully sampling storms less than 6 mm, which often produced little or no outflow. These smaller events that were not sampled can be assumed to have a high level of treatment since they were either stored in the SCM (i.e., long residence time) or exfiltrated to the underlying soil (i.e., providing further treatment before reaching the water table).

Although monitoring equipment was installed to measure drainage, it occurred only during events larger than 18.8 mm ($n = 7$ storms), and therefore only two drainage samples were obtained during the monitoring period. Assuming a 40% porosity in the AASHTO #4 aggregate of the IWS zone, a completely empty IWS zone would only capture (without drainage) the 11.4-mm event. During inter-event periods, the IWS zone quickly dewatered such that exfiltration occurred only from the scarified soil (5 cm thick) underling the aggregate (Winston *et al.* 2020). The dewatering of the IWS zone was caused by a leak in the cistern which allowed stormwater to move from the IWS zone through the backfilled soil and into the cistern, preventing drainage from occurring in 52 of 59 storm events, which is quite dissimilar to other studies of permeable pavements constructed over clayey soils (Fassman & Blackbourn 2010; Winston *et al.* 2018).

Runoff reduction in the treatment train stormwater control measure represented 27% of the overall water balance during the monitoring period (Winston *et al.* 2020). This was primarily due to exfiltration from scarified subgrade soil beneath the permeable pavement with minor contribution from leaks in the cistern causing it to partially dewater during inter-event periods. The drawdown rate from the scarified soil into the soil underlying the treatment train was 0.061 mm/hr (measured in a monitoring well located within the permeable pavement; Winston *et al.* 2020). Water in the scarified soil took approximately 16 days to exfiltrate completely; given the average dry period was 4.7 days, the scarified soil completely drained only once during the monitoring period. This meant that there was ample time for anaerobic conditions to form in the scarified soil during inter-event periods; Braswell *et al.* (2018) found these conditions develop within 36 hours of the cessation of rainfall.

Because runoff reduction resulted in moderation of pollutant loads draining directly into Old Woman Creek estuary, this portion of the pollutant load was eliminated from effluent load

Blue-Green Systems Vol 2 No 1
doi: 10.2166/bgs.2020.914

calculations. However, a fraction of this eliminated load will eventually discharge to the estuary as groundwater flow (Gallagher *et al.* 2018). Stormwater was never harvested from the cistern during the monitoring period, resulting in a lack of drawdown during inter-event periods and frequent overflow ($n = 45$ events) from the treatment train.

Water quality performance

Nutrient, chloride, and metals concentrations

The treatment train performed well for nutrient and sediment removal, particularly for sediment-bound pollutants (Table 1 and Figure 4). TKN and ON ERs were greater than 0.6, PBP and TP ERs were greater than 0.8, and TSS and turbidity ERs were greater than 0.95. Along with TN (ER = 0.54), these reductions were statistically significant. Median effluent concentrations of TN, TP, and TSS were low, with values of 0.87, 0.05, and 1 mg/L, respectively. The median effluent TN concentration is marginally higher than typical for SCMs employing biologically-based treatment

Table 1 | Summary statistics for nutrient and sediment concentrations at the asphalt (control), drainage, and cistern monitoring locations

Pollutant	Location	Units	*n*	Range	$\bar{x}$	$\tilde{x}$	*s*	CV	*p*-value	ER[a]	RE^{a}_{median}
TKN	Asphalt	mg/L	15	0.63–5.22	1.81	1.19	1.35	0.75	0.0068	**0.61**	**0.43**[b]
	Drainage		2	0.19–0.48	0.33	0.33	N/A	N/A			
	Cistern		15	0.4–1.15	0.70	0.67	0.21	0.29			
NO_2	Asphalt	mg/L	15	0.001–0.055	0.01	0.00	0.01	1.58	0.5015	− 3.59	0.41
	Drainage		2	0.003–0.006	0.00	0.00	N/A	N/A			
	Cistern		15	0–0.318	0.04	0.00	0.08	2.14			
NO_3	Asphalt	mg/L	15	0.03–0.55	0.18	0.12	0.16	0.87	0.1013	0.03	0.61
	Drainage		2	0.02–0.08	0.05	0.05	N/A	N/A			
	Cistern		15	0.02–1.16	0.18	0.05	0.30	1.68			
TN	Asphalt	mg/L	15	0.77–5.34	2.00	1.41	1.38	0.69	0.0036	**0.54**	**0.41**
	Drainage		2	0.28–0.51	0.39	0.39	N/A	N/A			
	Cistern		15	0.42–1.8	0.92	0.83	0.39	0.43			
TAN	Asphalt	mg/L	14	0–0.5	0.09	0.04	0.14	1.45	0.4055	0.11	− 0.45
	Drainage		2	0.011–0.02	0.01	0.01	N/A	N/A			
	Cistern		14	0.003–0.2	0.08	0.06	0.07	0.80			
ON	Asphalt	mg/L	13	0.6–5.18	1.61	0.85	1.35	0.84	0.0020	**0.62**	**0.33**
	Drainage		2	0.18–0.46	0.32	0.32	N/A	N/A			
	Cistern		13	0.37–1.14	0.61	0.57	0.21	0.35			
OP	Asphalt	mg/L	16	0.001–0.13	0.019	0.005	0.033	1.75	0.985	− 0.03	− 1.30
	Drainage		2	0.011–0.03	0.022	0.022	N/A	N/A			
	Cistern		16	0–0.05	0.019	0.012	0.020	1.05			
PBP	Asphalt	mg/L	15	0.03–0.92	0.28	0.18	0.25	0.92	1.55E − 5	**0.86**	**0.86**
	Drainage		2	0.03–0.05	0.04	0.04	N/A	N/A			
	Cistern		15	0–0.1	0.04	0.03	0.03	0.84			
TP	Asphalt	mg/L	15	0.03–0.93	0.29	0.24	0.25	0.86	0.0003	**0.80**	**0.71**
	Drainage		2	0.04–0.09	0.06	0.06	N/A	N/A			
	Cistern		15	0.01–0.1	0.06	0.07	0.03	0.51			
TSS	Asphalt	mg/L	16	41.2–3,025	450	198	731	1.62	2.55E − 14	**1.00**	**1.00**
	Drainage		2	4.4–8.5	6	6	N/A	N/A			
	Cistern		16	0.3–8.7	2	1	2	1.16			
Turbidity	Asphalt	NTU	15	7.37–1,323	157	35	339	2.16	1.15E − 8	**0.96**	**0.82**
	Drainage		2	6.82–9.99	8	8	N/A	N/A			
	Cistern		15	1.2–12.1	6	6	4	0.62			

[a]ER and RE_{median} were determined between the asphalt and cistern monitoring locations.
[b]Bolded parameters were significantly different between asphalt and cistern monitoring locations.

Blue-Green Systems Vol 2 No 1
doi: 10.2166/bgs.2020.914

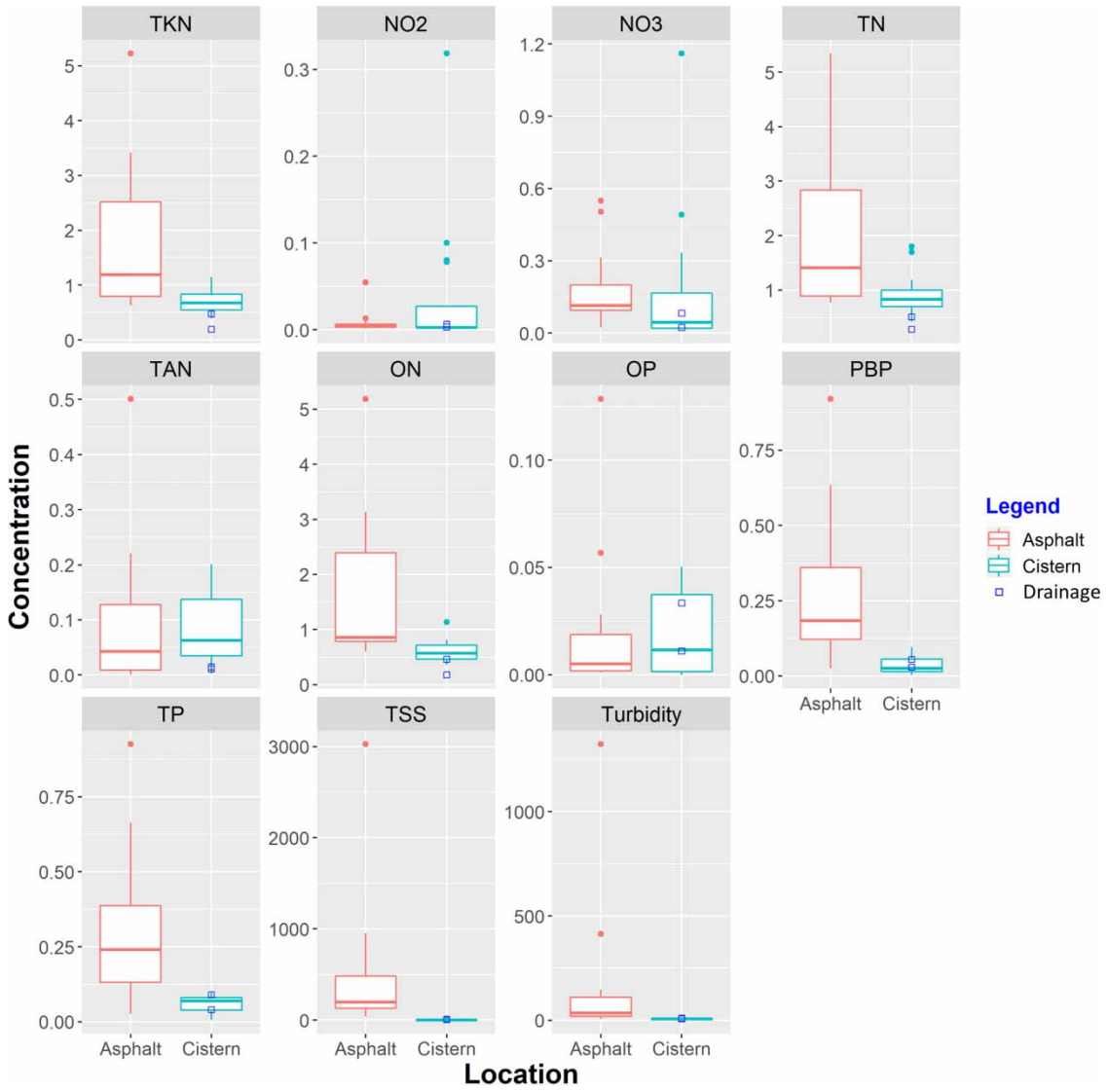

Figure 4 | Boxplots of nutrient, TSS, and turbidity concentrations from the asphalt and cistern monitoring locations. Drainage concentrations are plotted as open symbols superimposed over the cistern boxplot. Nutrient and TSS concentrations are in mg/L, while turbidity is measured in NTU (Nephelometric Turbidity Units). Each boxplot provides an indication of the interquartile range and the median value. The whiskers extend 150% further than the interquartile range. Outliers are shown as single, solid points.

mechanisms, such as bioretention, while the TP and TSS median effluent concentrations were lower than conventional SCMs reported in the literature (Winston *et al.* 2015). NO_2, TAN, and OP concentrations were not significantly different after stormwater passed through the treatment train. Based on the limited drainage data ($n = 2$ storms; Figure 4), it appears the majority of the pollutant removal occurred in the first SCM in the treatment train, similar to previous research (Barrett *et al.* 1998; Hathaway & Hunt 2009).

Filtration at the permeable pavement surface followed by sedimentation within the permeable pavement cross-section and cistern were the primary mechanisms for sediment removal. Other studies on permeable pavement and cisterns have shown substantial (often >50%) and significant reduction in sediment and sediment-bound pollutant concentrations (Collins *et al.* 2010; Kim & Han 2011; Roseen *et al.* 2012; DeBusk & Hunt 2014; Drake *et al.* 2014a).

Nitrate is highly mobile in soils and groundwater and can cause human health concerns such as methemoglobinemia. Nitrate concentrations typically increase substantially through permeable pavements when they are conventionally drained (i.e., underdrain at the bottom of the cross-section), since

Blue-Green Systems Vol 2 No 1
doi: 10.2166/bgs.2020.914

aerobic environments predominate (Collins *et al.* 2010; Roseen *et al.* 2012; Drake *et al.* 2014a). Under these conditions, the process of ammonia oxidation transforms TAN to NO_2^- which is followed by nitrate oxidation (together known as nitrification). These reactions are mediated by species of the genus *Nitrosomonas* and *Nitrobacter*, respectively. Optimum pH ranges for these bacteria are between 7.0 and 8.0 and 7.5 and 8.0, respectively (Shammas 1986), which are similar to the observed drainage pH (mean = 7.7). Similar to previous studies (Collins *et al.* 2010), transformation of TAN to NO_2^- probably occurred in this permeable pavement during rainfall events, when stormwater was (presumably) aerobic (Figure 4). Following the cessation of rainfall, long-term storage of water within the scarified soil beneath the permeable pavement (observed in the monitoring well stage data; Winston *et al.* 2020) caused anaerobic conditions and spurred denitrification and/or other anaerobic processes (e.g., dissimilatory nitrate reduction to ammonia [DNRA]; Figure 2). Mean nitrate concentrations in drainage were less than one-third those from the asphalt, and were significantly lower ($\alpha = 0.10$) through the treatment train.

Denitrification is microbially-mediated by heterotrophic bacteria and results in the production of N_2 gas from nitrate. Denitrification requires a carbon source and occurs optimally at pH 7–8 (Gumaelius *et al.* 1996). In this case, the dissolved and particulate organic matter in the stormwater apparently provided enough carbon for denitrifying bacteria to thrive, since little organic matter is expected in the soil underlying the permeable pavement (B horizon). Denitrification has been observed in a permeable pavement employing IWS (Braswell *et al.* 2018); this occurred in the 72 hours following a storm event, during which the dissolved oxygen present in stormwater declined due to aerobic bacterial respiration. It is theorized that similar processes are occurring in the permeable pavement studied herein, suggesting that an additional carbon source beyond that found in stormwater is not needed for denitrification to occur in the scarified soil beneath permeable pavements.

In the permeable pavement studied herein, we postulate that the influx of dissolved oxygen in stormwater created an aerobic environment intra-event, driving TAN to NO_2^- to NO_3^-. Inter-event denitrification reduced NO_2^- and NO_3^- concentrations, and the water stored in the scarified soil mixed with incoming stormwater, diluting asphalt NO_2^- and NO_3^- concentrations substantially by the time drainage occurred.

Drainage and cistern water quality was generally similar. Water in the cistern appeared to be aerobic immediately after rainfall events, as ON appears to have been mineralized to TAN. Further oxidation to NO_2^- may have occurred, as the nitrite ER was −3.59 for the treatment train. Nitrification drives pH lower as H^+ ions are released into solution, potentially resulting in 1–1.5 units lower pH in the cistern than in drainage samples. Nitrate concentrations in the cistern were similar to those in drainage samples (Figure 4).

On average, asphalt runoff TP was 97% sediment-bound, resulting in excellent TP retention (ER = 0.80). As with TSS, the vast majority of the TP and PBP reduction was provided by the permeable pavement. OP, the dissolved and most bioavailable form of P, was not well controlled by the treatment train SCM (ER = −0.03). Similar performance has been observed in other permeable pavement and cistern studies (Drake *et al.* 2014a; Wilson *et al.* 2014; Winston *et al.* 2016b). At concentrations similar to those herein (<0.02 mg/L), very little sorption of OP to the limestone aggregate would be expected (Zhou & Li 2001). The incorporation of water treatment residuals or other Fe and Al oxide containing materials in SCMs could be utilized to potentially reduce OP (O'Neill & Davis 2011), albeit OP concentrations from the asphalt may be near irreducible levels (Strecker *et al.* 2001).

Concentrations of total Al, Fe, and Mn were significantly and substantially (>70%) reduced through the treatment train, suggesting particulate capture within the system (further supported by the significant sediment sequestration observed; Table 2). Al and Fe were reduced by 20–60% in a permeable pavement monitoring study in Canada (Drake *et al.* 2014a). No significant differences for Cu, Pb, and Zn ERs were observed and ERs were −0.19. −0.39, and 0.17, suggesting that these pollutants were not well retained. ERs for these pollutants in previous permeable pavement studies typically

Blue-Green Systems Vol 2 No 1
doi: 10.2166/bgs.2020.914

Table 2 | Summary statistics for chloride, metals, silicate, sulfate, total alkalinity, and pH at the asphalt (control), drainage, and cistern monitoring locations

Pollutant	Location	Units	*n*	Range	$\bar{x}$	$\tilde{x}$	*s*	CV	*p*-value	ER[a]	RE^{a}_{median}
Cl	Asphalt	mg/L	16	0–1.89	0.3	0	0.5	1.70	2.28E − 6	**− 29.7**[b]	**N/A**[c]
	Drainage		2	1.31–2.23	1.8	1.8	N/A	N/A			
	Cistern		16	0.68–35.52	9	4	11.3	1.21			
Al	Asphalt	μg/L	15	82–13,550	2,051	363	3,730	1.82	0.0289	**0.88**	**0.47**
	Drainage		2	122–274	198	198	N/A	N/A			
	Cistern		15	75–526	252	193	147	0.58			
Ca	Asphalt	μg/L	15	11,680–152,000	39,873	26,190	39,436	0.99	0.0043	**− 0.54**	**− 0.18**
	Drainage		2	17,120–17,830	17,475	17,475	N/A	N/A			
	Cistern		15	24,580–133,700	61,581	31,030	40,427	0.66			
Cu	Asphalt	μg/L	15	3.17–22.51	9.39	8.55	5.80	0.62	0.1156	− 0.19	− 0.06
	Drainage		2	2.78–3.69	3.24	3.24	N/A	N/A			
	Cistern		15	2.57–30.64	11.22	9.09	8.46	0.75			
Fe	Asphalt	μg/L	15	118–21,450	3,188	683	5,798	1.82	0.0071	**0.91**	**0.68**
	Drainage		2	128–269	198	198	N/A	N/A			
	Cistern		15	151–576	299	217	143	0.48			
Mg	Asphalt	μg/L	15	1,129–29,260	7,232	3,622	8,455	1.17	0.0066	**− 1.00**	**− 0.76**
	Drainage		2	3,217–3,336	3,277	3,277	N/A	N/A			
	Cistern		15	5,506–32,430	14,467	6,375	10,247	0.71			
Mn	Asphalt	μg/L	15	12.7–661.6	146	78	172	1.18	0.0049	**0.73**	**0.56**
	Drainage		2	3.97–7.41	6	6	N/A	N/A			
	Cistern		15	3.96–131.8	39	34	30	0.77			
Pb	Asphalt	μg/L	15	0.35–26.04	4.59	2.13	6.70	1.46	0.8450	− 0.39	− 0.25
	Drainage		2	0.18–0.32	0.25	0.25	N/A	N/A			
	Cistern		15	0.4–58.95	6.37	2.66	14.66	2.30			
Zn	Asphalt	μg/L	15	14–1,080	153	79	269	1.76	0.3742	0.17	− 0.31
	Drainage		2	4–6	5	5	N/A	N/A			
	Cistern		15	14–309	127	104	87	0.68			
Total alkalinity	Asphalt	mg/L	16	15.2–61.5	31	28	12	0.39	5.57E − 6	**− 1.70**	**− 2.31**
	Drainage		2	46.9–48	47	47	N/A	N/A			
	Cistern		16	36.6–110.5	83	92	26	0.31			
Silicate	Asphalt	mg/L	16	0.1–1.01	0.44	0.39	0.24	0.54	1.54E − 6	**− 10.40**	**− 12.91**
	Drainage		2	2.83–6.92	4.88	4.88	N/A	N/A			
	Cistern		16	2.4–7.59	5.03	5.47	2.17	0.43			
Sulfate	Asphalt	mg/L	11	1.87–4.64	2.8	2.6	0.82	0.29	5.67E − 6	**− 12.75**	**− 2.49**
	Drainage		2	8.31–8.37	8.3	8.3	N/A	N/A			
	Cistern		11	3.96–138.5	38.8	9.1	54.26	1.40			
pH	Asphalt	unitless	8	6.43–7.56	7.2	7.4	0.43	0.06	0.0092	**0.11**	**0.15**
	Drainage		2	7.7–7.75	7.7	7.7	N/A	N/A			
	Cistern		7	6.06–6.81	6.4	6.4	0.28	0.04			

[a]ER and RE_{median} were determined between the asphalt and cistern monitoring locations.
[b]Bolded parameters were significantly different between asphalt and cistern monitoring locations.
[c]RE_{median} could not be calculated due to median influent concentration value of 0 mg/L.

range from 0.6–0.8 (Brattebo & Booth 2003; Roseen *et al.* 2012; Drake *et al.* 2014a). While cistern metals ERs were not available in the literature, effluent concentrations of Cu, Pb, and Zn from rainwater harvesting systems in Australia (mean of 160, 10, and 230 μg/L, respectively) were, in most cases, similar to those for the cistern monitoring point herein (mean of 11, 6, and 127 μg/L, respectively; Kus *et al.* 2010). Effluent metals concentrations from the treatment train were well below human health protection thresholds set for recreational uses (ANZECC 2000). While asphalt runoff concentrations were sometimes above drinking water standards, median effluent concentrations from the SCM were below these standards for the United States (USEPA 2009).

Blue-Green Systems Vol 2 No 1
doi: 10.2166/bgs.2020.914

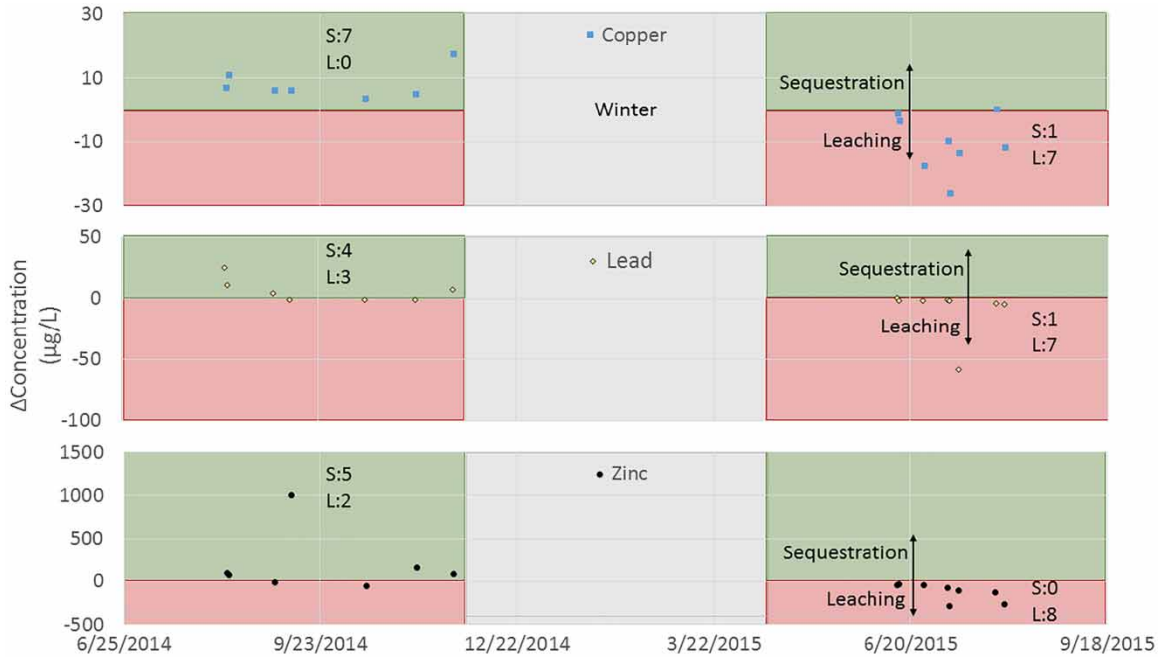

Figure 5 | Change in concentration of copper, lead, and zinc from asphalt to cistern monitoring locations. The number of events with metal sequestration (S) and leaching (L) during 2014 and 2015 are shown.

The lack of sequestration of Cu, Pb, and Zn during 2015 was perhaps caused by several factors (Figure 5): (1) moderating of asphalt runoff concentrations with time, (2) a decrease in pH in the cistern (Table 2), which may cause de-sorption of metals (Despins *et al.* 2009), and (3) de-sorption of metals from sediment in the cistern due to the application of NaCl (deicing salt) in winter (Bäckström *et al.* 2004). Although metal speciation was not analyzed, drainage concentrations (albeit only $n = 2$) indicated the permeable pavement trapped Cu, Pb, and Zn; this combined with cistern TSS concentrations ($\bar{x} = 2$ mg/L) probably meant that dissolved Cu, Pb, and Zn were leached. Two potential reasons for this exist: (1) leaching of metals as de-sorption occurs from accumulated sediment in the cistern or (2) interaction with plumbing fixtures (pump, spigot, metal fittings and pipe) inherent to the supply line (Figure 1), which have been shown to be potential sources of heavy metals (Morrow *et al.* 2010).

The significant export of Ca and Mg (ER of −0.54 and 1.0, respectively) from the treatment train is related both to the aggregate underlying the permeable pavement and the concrete cistern. Quarried rock in north-central Ohio is typically dolomitic limestone, made up of limestone ($CaCO_3$) and dolomite [$CaMg(CO_3)_2$], which leach Ca and Mg ions to water (Lamar & Shorde 1953). Ca and Mg concentrations increased by 50% and doubled, respectively, from the asphalt to the drainage monitoring location ($n = 2$). Concentrations of both analytes approximately doubled again during storage in the cistern; with as little as 24 hr contact time, substantial Ca and Mg (10^4–10^5 mg/kg concrete) leaching from concrete has been observed (Martens *et al.* 2010), especially at neutral or acidic pH (mean pH was 6.43 in the cistern). Calcium and magnesium oxides make up substantial fractions of both cement and fly ash (Haque & Kayyali 1995).

Chloride concentrations in parking lot runoff were always less than 2 mg/L and were BDL in more than half of the sampled events ($n = 10/16$). Since all sampled storms occurred in the summer and autumn, no appreciable residual salt remained in the watershed, as a minimum of 2.5 months had elapsed since the previous snowfall. Chloride concentrations significantly increased through the treatment train (ER = −29.7), from a mean of 0.31 mg/L in asphalt samples to 1.77 mg/L in drainage samples to 9.38 mg/L in cistern samples. This suggested that residual chloride from deicing salt was present in both the permeable pavement and cistern, but that the cistern was the primary

Blue-Green Systems Vol 2 No 1
doi: 10.2166/bgs.2020.914

source of chloride. However, the maximum observed cistern concentration (33 mg/L) was well below both the acute (860 mg/L) and chronic (230 mg/L) toxicity levels for chloride (USEPA 2012). Observed cistern concentrations were also at least a factor of ten lower than recommended maximum chloride concentrations for water used to irrigate turfgrass (Fipps 2016); thus, the water could safely be harvested for landscape irrigation, particularly in the summer when several months have passed since the last deicing salt application.

Chloride release from permeable pavements in cold climates has been observed year-round, with a power regression describing the relationship between chloride in drainage samples and elapsed time since the previous snowfall (Borst & Brown 2014). Drake *et al.* (2014b) and Winston *et al.* (2016b) also observed that permeable pavement leached chloride to runoff. Sources of chloride from this treatment train include leaching from dolomitic aggregate of the permeable pavement (Lamar & Shorde 1953), residual chloride from deicing salt, and the concrete cistern itself. $CaCl_2$ or NaCl admixtures are often used to improve concrete strength and reduce curing time. Haque & Kayyali (1995) showed that substantial chloride leaching can occur in as little as 24 hrs contact time between concrete and water.

Median alkalinity of the influent runoff was 28 mg/L, increasing to 48 mg/L in drainage samples, and 92 mg/L in the cistern. This increase was significant through the treatment train. This suggests that buffering capacity of the stormwater increased as it interacted with the concrete pavers, underlying dolomitic limestone aggregate, and concrete cisterns. Both concrete and limestone are known sources of carbonate (Clifton 1993), which directly translate to increases in alkalinity. Substantial (in some cases more than 30-fold) and significant increases in total alkalinity were reported after 100 minutes of recirculation of runoff through concrete pipes (Davies *et al.* 2010). A linear increasing trend ($R^2 = 0.83$, slope $= 0.16$) in effluent total alkalinity from the treatment train was observed with time, suggesting buffering capacity was increasing with time, while influent and drainage total alkalinity remained consistent throughout the monitoring period. Concomitant increasing linear trends in effluent TAN, OP, and silicate were observed with time (R^2 from 0.51 to 0.86). Similar trends in effluent sulfate concentration or pH were not observed, perhaps because these parameters were only measured in 2015, reducing the potential to observe temporal trends. Increases in alkalinity and parameters contributing to it through the treatment train are not unexpected given that contact time has been positively correlated to increased alkalinity in other studies (e.g., Wolock *et al.* 1989).

pH increased through the permeable pavement cross-section, with mean drainage pH approximately 0.5 units higher than asphalt runoff (7.7 and 7.2, respectively; Table 2 and Figure 6). This is consistent with results from Collins *et al.* (2010), where pH of slightly acidic rainfall (6.7) increased to approximately 8.0 after passing through PICP. Interestingly, median effluent pH significantly decreased to 6.36 after stormwater passed into the concrete cistern, which contrasts with past research on urban runoff interactions with concrete pipes and changes in water chemistry (Davies *et al.* 2010), where significant pH increases were observed. Perhaps this decrease in pH is related to observed nitrification in the cistern (Figure 4).

Effluent alkalinity was elevated compared to asphalt runoff, exhibiting a linear, inverse relationship to pH ($R^2 = 0.59$, slope $= -0.05$). This inverse relationship is unusual but not unprecedented (Freeze & Cherry 1979; Piñol & Avila 1992); when water is supersaturated with calcite, the pH-alkalinity relationship is governed by the solubility equilibrium of calcite. In the present case, stormwater interactions with the dolomitic limestone aggregate and concrete were both sources of calcite, which is supported by the substantial and significant increases in Ca through the treatment train.

Stormwater in the cistern was not exposed to light, meaning that photosynthetic organisms were not active, ceding respiration to microbes that do not release new bicarbonate ions (H_2CO_3) into solution. Because sulfate concentration substantially increased from asphalt runoff to effluent (median 2.6 mg/L

Blue-Green Systems Vol 2 No 1
doi: 10.2166/bgs.2020.914

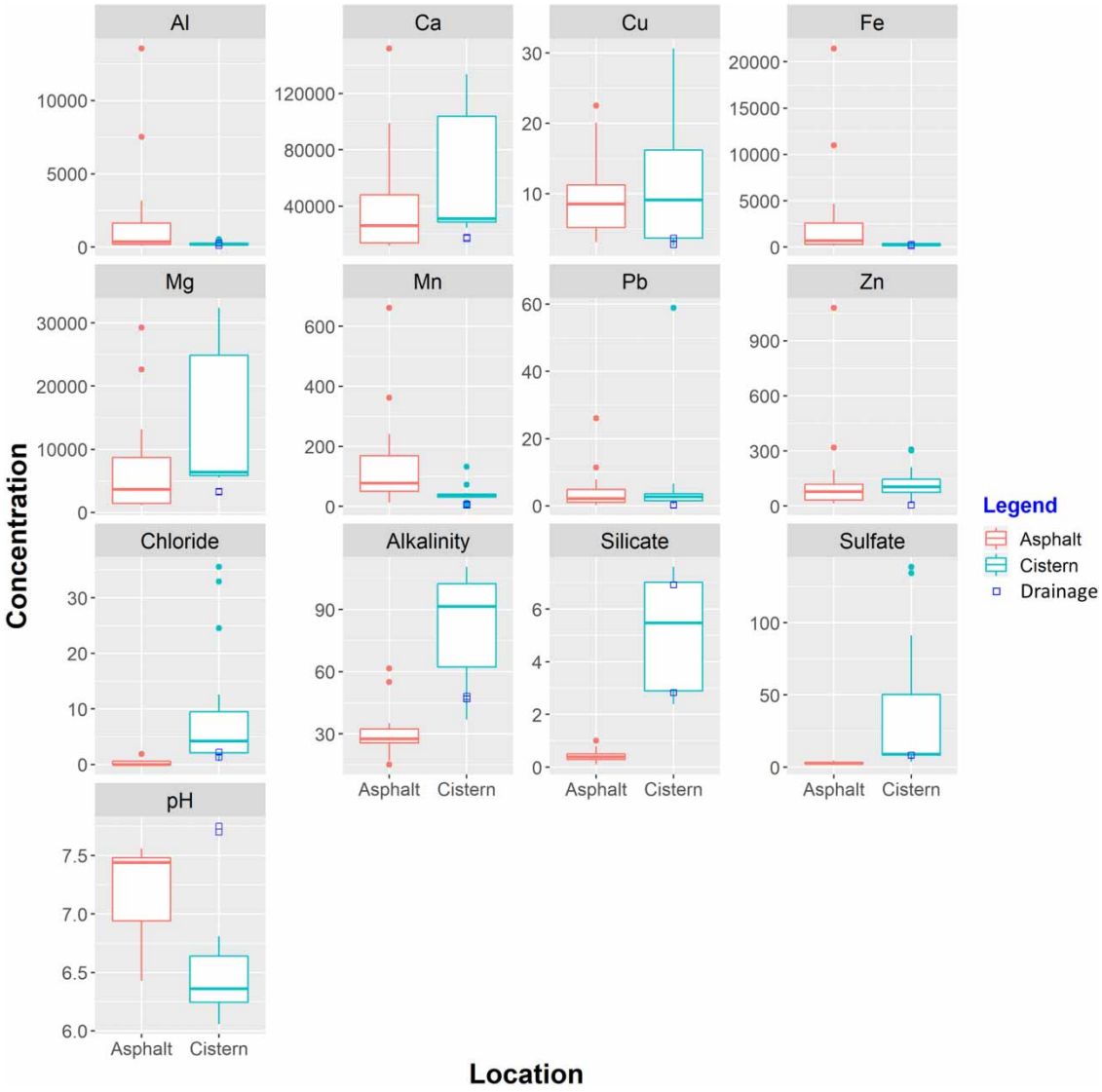

Figure 6 | Boxplots of pH, metals, chloride, alkalinity, silicate, and sulfate concentrations for the asphalt and cistern monitoring locations. Drainage concentrations are plotted as open symbols superimposed over the cistern boxplot. Aluminum, calcium, copper, iron, magnesium, manganese, lead, and zinc concentrations are in μg/L. Chloride, alkalinity, silicate, and sulfate concentrations are in mg/L. pH is unitless. Each boxplot provides an indication of the interquartile range and the median value. The whiskers extend 150% further than the interquartile range. Outliers are shown as single, solid points.

to 9.1 mg/L), sulfide oxidation occurred (alongside nitrification), concurrently decreasing pH:

$$S^0 + 1.5O_2 + H_2O \rightleftharpoons SO_4^{2-} + 2H^+ \quad \text{sulfur oxidation;} \tag{6}$$

During several dry periods, the access port to the cistern was opened and a distinct 'rotten egg' odor was noted, confirming anaerobic conditions in the cistern. Sulfate produced under aerobic conditions was reduced by dissimilatory sulfate reduction and eventually released as hydrogen sulfide gas (H_2S), producing this smell. This process concomitantly increases alkalinity (also observed in the cistern) by reducing sulfate and consuming organic acids (Braissant *et al.* 2007). Optimal conditions for this process are pH 6–8, with cistern pH ranging from 6.1–6.8 (O'Flaherty *et al.* 1998; Jong & Parry 2006).

Blue-Green Systems Vol 2 No 1
doi: 10.2166/bgs.2020.914

Pollutant loads

Coupling modest runoff reduction (27%) with pollutant transformations, filtration, and sedimentation within the treatment train led to significant load reduction of TSS (99.5%) and nutrients which are primarily particulate-bound (Table 3). For instance, TKN, ON, and PBP SOLs were all greater than 60%. This performance was similar to particulate and particulate-bound pollutant load reductions from previous studies of permeable pavements (Drake *et al.* 2014a; Winston *et al.* 2016b), suggesting that the permeable pavement is providing the majority of the load reduction in the treatment train. This corroborates evidence in Hathaway & Hunt (2009) that the first SCM in a treatment train provides the majority of the pollutant removal.

Total nitrogen and TP loads were significantly reduced by 59 and 78%, respectively. Dissolved P is a key contributor to algal blooms in eutrophic water bodies worldwide (Correll 1998), but OP loads increased by 76% (not statistically significant) through the treatment train. This is probably due to an extremely low influent concentration (median = 0.005 mg/L) which may have been irreducible based on the unit processes in the treatment train; the median effluent concentration of OP (0.01 mg/L) was (1) very low and (2) similar to the best performing bioretention cells in the literature (Passeport *et al.* 2009; Brown & Hunt 2011). Significant load reduction for aqueous forms of nitrogen (NO_2, NO_3, and TAN) was not observed, similar to other studies on permeable pavement and rainwater harvesting SCMs (Roseen *et al.* 2012; Wilson *et al.* 2014; Winston *et al.* 2016b). The treatment train in this study performed better than most permeable pavements regarding nitrate load, which often increases due to nitrification in the pavement cross-section (Drake *et al.* 2014a). This may be due to aforementioned denitrification during inter-event periods resulting from long-term storage of water in the scarified soil underlying the permeable pavement (Figure 2).

The treatment train SCM did not significantly affect pollutant loading of Ca, Mg, Cu, Pb, or Zn (Table 3). The latter three metals are particularly surprising, given previous permeable pavement studies showing pollutant load reduction for these pollutants (Brattebo & Booth 2003; Roseen *et al.* 2012). Non-significant Ca and Mg load increases were probably related to leaching of Ca^{2+} and Mg^{2+} from the dolomitic limestone aggregate. Eighty to 90% load reductions occurred for Al, Fe, and Mn. Chloride loads increased nearly 40-fold through the treatment train, which can be attributed to latent chloride from winter salting or leaching from concrete or limestone (Borst & Brown 2014). Most SCMs in cold climates are sources rather than sinks of chloride (Roseen *et al.* 2012; Borst & Brown 2014; Winston *et al.* 2016b), reflecting anthropogenic addition of deicing salt and subsequent leaching from SCMs for months following application. Total alkalinity, silicate, and sulfate load increased (the latter two significantly) through the treatment train. Sulfate was produced in the cistern through sulfide oxidation, while the observed substantial increases in alkalinity and silicate are both related to interactions between the stormwater and concrete, which contains substantial carbonate and silicate minerals (Clifton 1993). Annual loading trends for the treatment train were similar to SOL trends (Table 3).

Overall, this treatment train SCM showed promise for reduction of pollutant loading in parking lot runoff prior to discharge to surface water bodies. For instance, TN, TP, and TSS loads were reduced by 59, 78, and 99.5%, similar to the best performing bioretention cells and permeable pavement systems in the literature (Davis 2007; Passeport *et al.* 2009; Collins *et al.* 2010; Drake *et al.* 2014a). Lessons learned suggest load reduction could be improved by: (1) use of the stormwater stored in the cistern to provide storage for oncoming storm events, (2) purposeful design of the cistern with a passive drawdown device (Gee & Hunt 2016), (3) decreasing the run-on ratio, (4) ongoing maintenance of the permeable pavement and cistern, and (5) providing a carbon source in the permeable pavement cross-section to spur greater denitrification during inter-event periods.

Table 3 | Cumulative loading, summation of load (SOL), and annual loading (kg/ha/yr) for nutrients, sediment, metals, alkalinity, chloride, silicate, and sulfate for the treatment train stormwater control measure

Pollutant	TKN		Nitrite		Nitrate		TN		TAN		ON		TP		OP		PBP		TSS		Total Alkalinity	
Monitoring Location	Asp.[a]	Eff.[b]	Asp.	Eff.	Asp.	Eff.	Asp.	Eff.	Asp.	Eff.	Asp.	Eff.	Asp.	Eff.	Asp.	Eff.	Asp.	Eff.	Asp.	Eff.	Asp.	Eff.
Cumulative Loading (kg)	0.17	0.059	0.001	0.002	0.021	0.02	0.19	0.082	0.006	0.007	0.14	0.045	0.029	0.006	0.001	0.002	0.028	0.004	43.05	0.21	3.36	7.41
SOL (%)	6.60**[c]		− 80		9		59**		− 13		66**		78**		− 76		85***		99.5***		− 121	
Annual Loading (kg/ha/yr)	3.16	1.04	0.01	0.02	0.35	0.2	3.67	1.35	0.11	0.11	2.4	0.85	0.59	0.11	0.02	0.03	0.5	0.06	653.5	2.6	68	137
Pollutant	**Al**		**Ca**		**Cu**		**Fe**		**Mg**		**Mn**		**Pb**		**Zn**		**Cl**		**Silicate**		**Sulfate**	
Monitoring Location	Asp.	Eff.	Asp.	Eff.	Asp.	Eff.	Asp.	Eff.	Asp.	Eff.	Asp.	Eff.	Asp.	Eff.	Asp.	Eff.	Asp.	Eff.	Asp.	Eff.	Asp.	Eff.
Cumulative Loading (kg)	0.18	0.02	3.97	4.88	0.001	0.001	0.28	0.029	0.72	1.1	0.01	0.003	0.0004	0.0004	0.024	0.012	0.02	0.79	0.06	0.45	0.27	1.26
SOL (%)	88*		− 23		− 25		89**		− 52		79**		3		48		− 3,977***		− 644***		− 368**	
Annual Loading (kg/ha/yr)	2,093	343	71,628	66,759	20.3	17.4	3,378	427	11,373	14,516	229	52	6.67	5.64	316	188	0.2	10.1	1.1	8.3	6	18.1

[a]Asphalt runoff (representative of inflow to treatment train).
[b]Effluent from treatment train.
[c]*$p < 0.05$, **$p < 0.01$, ***$p < 0.001$.

doi: 10.2166/bgs.2020.914

Blue-Green Systems Vol 2 No 1
doi: 10.2166/bgs.2020.914

A year-round, consistent, and electronically controlled use for harvested stormwater has been shown effective in dewatering cisterns. Automated release of stored water from a cistern in advance of a storm event can improve its stormwater management benefits (Gee & Hunt 2016; Xu *et al.* 2018). Decreasing the run-on ratio increases the relative void storage in the aggregate beneath the permeable pavement and decreases maintenance burden. Of particular importance is the storage (either in an IWS zone or in scarified soil) below the underdrain invert, since this is responsible for the majority of exfiltration observed in low K_{sat} soils. While no surface runoff was observed from the permeable pavement in this case, eliminating it through proper maintenance is key to maximizing pollutant load reduction. Finally, periodic maintenance of the cistern is needed to prevent re-suspension or leaching of dissolved metals from accumulated sediment.

SUMMARY AND CONCLUSIONS

A permeable pavement and stormwater harvesting treatment train SCM was constructed at the Old Woman Creek National Estuarine Research Reserve visitor center parking lot in Huron, Ohio, in June–July, 2014. Thirteen months of extensive hydrologic and water quality monitoring ensued. The following conclusions were drawn from this study:

1. Particulates were very well retained through filtration at the pavement surface and settling in the treatment train cross-section. TSS and turbidity were reduced by a minimum of 96%, with TSS load reduced by 99.5%. Organic nitrogen, TKN, TN, PBP, and TP concentrations were all significantly reduced by more than 40%. Median effluent phosphorus (total and dissolved) and TSS concentrations from this treatment train were lower than those reported in the literature for conventional SCMs, e.g. bioretention, wet ponds, and permeable pavements.
2. Dissolved nutrient species are often difficult to sequester from stormwater runoff, but significant reduction ($\alpha = 0.10$ level) of NO_3^- was observed for the treatment train. Based on effluent concentrations from drainage and cistern samples, it is evident that this treatment was primarily provided by the permeable pavement. Because stormwater was constantly stored in the scarified soil beneath the permeable pavement, anaerobic conditions formed during inter-event periods, spurring denitrification. This study suggests that there may be enough dissolved and particulate organic matter in stormwater to provide a carbon source for denitrification in the permeable pavement cross-section, corroborating findings from Braswell *et al.* (2018).
3. Given the excellent particulate capture, a high level of sequestration of particulate-bound metals was expected. However, no significant treatment effect was observed for total Cu, Pb, and Zn concentrations. During the first few months, sequestration of these pollutants was observed, but following a monitoring hiatus during winter snow and ice, leaching of these pollutants occurred. It is theorized this is most likely related to the use of chloride deicers or the decrease in pH within the cistern, which would cause metals to de-sorb from particulate matter in the cistern.

The long-term performance of this treatment train is predicated on maintenance of the permeable pavement to ensure its hydraulic functionality and of the cistern to remove accumulated sediments. Treatment train performance could have been substantially improved through consistent, dedicated, and year-round uses for the stormwater in the cistern or through passive or active release of detained stormwater from the cistern to provide storage for future storm events. Since stormwater was not harvested during the study period, it is difficult to extend the water quality performance herein to a similar system where cistern water is utilized during inter-event periods; however, promoting use of harvested stormwater will reduce effluent loading to receiving surface waters. Overall, this treatment train shows potential to improve urban runoff quality and to provide pretreatment for stormwater harvesting schemes.

Blue-Green Systems Vol 2 No 1
doi: 10.2166/bgs.2020.914

ACKNOWLEDGEMENTS

This work was partially supported by the University of New Hampshire under Cooperative Agreement No. NA09NOS4190153 (CFDA No. 11.419) from the National Oceanic and Atmospheric Association and by the United States Environmental Protection Agency Center for Comprehensive, optimaL, and Effective Abatement of Nutrients (CLEAN) [EPA Grant Number RD835570]. This work was also supported by Oldcastle Infrastructure through donation of the PICP and the precast concrete vaults. Any opinions, findings, and conclusions or recommendations expressed in this publication are those of the author(s) and do not necessarily reflect the views of the University of New Hampshire, the National Oceanic and Atmospheric Association, Oldcastle Infrastructure, or the United States Environmental Protection Agency.

The authors wish to thank the staff of the Old Woman Creek National Estuarine Research Reserve for their support throughout the project, particularly Frank Lopez and Heather Elmer. Additionally, graduate students at the University of New Hampshire (Rebecca Jacobson and Will Brown) contributed to construction supervision and data collection. The laboratory staff at both the Northeast Ohio Regional Sewer District and Old Woman Creek National Estuarine Research Reserve are appreciated for the analysis of water quality samples during the project.

REFERENCES

ANZECC & ARMCANZ 2000 *Australian and New Zealand Guidelines for Fresh and Marine Water Quality: Volume 2 – Aquatic Ecosystems – Rationale and Background Information*. Australian and New Zealand Environment and Conservation Council (ANZECC), Agriculture and Resource Management Council of Australia and New Zealand. Available: https://www.environment.gov.au/system/files/resources/53cda9ea-7ec2-49d4-af29-d1dde09e96ef/files/nwqms-guidelines-4-vol1.pdf.

APHA, AWWA, WEF 2012 *Standard Methods for the Examination of Water and Wastewater* (Bridgewater, L., ed.), 22nd edn. American Public Health Association (APHA), American Water Works Association (AWWA), and Water Environment Federation (WEF), Washington, DC.

Bäckström, M., Karlsson, S., Bäckman, L., Folkeson, L. & Lind, B. 2004 Mobilisation of heavy metals by deicing salts in a roadside environment. *Water Research* **38** (3), 720–732.

Bannerman, R. T., Owens, D. W., Dodds, R. B. & Hornewer, N. J. 1993 Sources of pollutants in Wisconsin stormwater. *Water Science and Technology* **28** (3), 241–259.

Barrett, M. E., Walsh, P. M., Malina, J. F. & Charbeneau, R. J. 1998 Performance of vegetative controls for treating highway runoff. *Journal of Environmental Engineering* **124** (11), 1121–1128.

Borst, M. & Brown, R. A. 2014 Chloride released from three permeable pavement surfaces after winter salt application. *Journal of the American Water Resources Association* **50** (1), 29–41.

Braissant, O., Decho, A. W., Dupraz, C., Glunk, C., Przekop, K. M. & Visscher, P. T. 2007 Exopolymeric substances of sulfate-reducing bacteria: interactions with calcium at alkaline pH and implication for formation of carbonate minerals. *Geobiology* **5** (4), 401–411.

Braswell, A. P., Winston, R. J. & Hunt, W. F. 2018 Hydrologic and water quality performance of permeable pavement with internal water storage over a clay soil in Durham, North Carolina. *Journal of Environmental Management* **224**, 277–287.

Brattebo, B. O. & Booth, D. B. 2003 Long-term stormwater quantity and quality performance of permeable pavement systems. *Water Research* **37** (18), 4369–4376.

Brown, R. A. & Hunt, W. F. 2011 Underdrain configuration to enhance bioretention exfiltration to reduce pollutant loads. *Journal of Environmental Engineering* **137** (11), 1082–1091.

Clifton, J. R. 1993 Predicting the service life of concrete. *Materials Journal* **90** (6), 611–617.

Collins, K. A., Hunt, W. F. & Hathaway, J. M. 2010 Side-by-side comparison of nitrogen species removal for four types of permeable pavement and standard asphalt in eastern North Carolina. *Journal of Hydrologic Engineering* **15** (6), 512–521.

Correll, D. L. 1998 The role of phosphorus in the eutrophication of receiving waters: a review. *Journal of Environmental Quality* **27** (2), 261–266.

Davies, P. J., Wright, I. A., Jonasson, O. J. & Findlay, S. J. 2010 Impact of concrete and PVC pipes on urban water chemistry. *Urban Water Journal* **7** (4), 233–241.

Davis, A. P. 2007 Field performance of bioretention: water quality. *Environmental Engineering Science* **24** (8), 1048–1064.

Davis, A. P., Shokouhian, M. & Ni, S. 2001 Loading estimates of lead, copper, cadmium, and zinc in urban runoff from specific sources. *Chemosphere* **44** (5), 997–1009.

Blue-Green Systems Vol 2 No 1
doi: 10.2166/bgs.2020.914

DeBusk, K. M. & Hunt, W. F. 2014 Impact of rainwater harvesting systems on nutrient and sediment concentrations in roof runoff. *Water Science and Technology: Water Supply* **14** (2), 220–229.

Despins, C., Farahbakhsh, K. & Leidl, C. 2009 Assessment of rainwater quality from rainwater harvesting systems in Ontario. *Canada. Journal of Water Supply: Research and Technology* **58** (2), 117–134.

Doan, L. N. & Davis, A. P. 2017 Bioretention–cistern–irrigation treatment train to minimize stormwater runoff. *Journal of Sustainable Water in the Built Environment* **04017003**, 1–10.

Drake, J., Bradford, A. & Van Seters, T. 2014a Stormwater quality of spring–summer-fall effluent from three partial-infiltration permeable pavement systems and conventional asphalt pavement. *Journal of Environmental Management* **139**, 69–79.

Drake, J., Bradford, A. & Van Seters, T. 2014b Winter effluent quality from partial-infiltration permeable pavement systems. *Journal of Environmental Engineering* **140**, 11.

Fassman, E. A. & Blackbourn, S. 2010 Urban runoff mitigation by a permeable pavement system over impermeable soils. *Journal of Hydrologic Engineering* **15** (6), 475–485.

Freeze, R. A. & Cherry, J. A. 1979 *Groundwater*. Prentice-Hall, Englewood Cliffs, NJ.

Fipps, G. 2016 Irrigation water quality standard and salinity management. Texas A&M Agrilife Extension, B-1667, College Station, TX.

Gallagher, K. C., Alsharif, K., Tsegaye, S. & Van Beynen, P. 2018 A new approach for using GIS to link infiltration BMPs to groundwater pollution risk. *Urban Water Journal* **15** (9), 847–857.

Gee, K. D. & Hunt, W. F. 2016 Enhancing stormwater management benefits of rainwater harvesting via innovative technologies. *Journal of Environmental Engineering* **142** (8), 04016039.

Gomez-Ullate, E., Novo, A. V., Bayon, J. R., Hernandez, J. R. & Castro-Fresno, D. 2011 Design and construction of an experimental pervious paved parking area to harvest reusable rainwater. *Water Science and Technology* **64** (9), 1942–1950.

Gumaelius, L., Smith, E. H. & Dalhammar, G. 1996 Potential biomarker for denitrification of wastewaters: effects of process variables and cadmium toxicity. *Water Research* **30** (12), 3025–3031.

Haque, M. N. & Kayyali, O. A. 1995 Free and water soluble chloride in concrete. *Cement and Concrete Research* **25** (3), 531–542.

Hathaway, J. M. & Hunt, W. F. 2009 Evaluation of storm-water wetlands in series in Piedmont North Carolina. *Journal of Environmental Engineering* **136** (1), 140–146.

Jong, T. & Parry, D. L. 2006 Microbial sulfate reduction under sequentially acidic conditions in an upflow anaerobic packed bed bioreactor. *Water Research* **40** (13), 2561–2571.

Kim, M. & Han, M. 2011 Composition and distribution of bacteria in operating rainwater harvesting tank. *Water Science and Technology* **63** (7), 1524–1530.

Kus, B., Kandasamy, J., Vigneswaran, S. & Shon, H. K. 2010 Water quality characterisation of rainwater in tanks at different times and locations. *Water Science and Technology* **61** (2), 429–439.

Lamar, J. E. & Shorde, R. S. 1953 Water soluble salts in limestone and dolomites. *Economic Geology* **48** (2), 97–112.

Legret, M. & Colandini, V. 1999 Effects of a porous pavement with reservoir structure on runoff water: water quality and fate of heavy metals. *Water Science and Technology* **39** (2), 111–117.

Martens, E., Jacques, D., Van Gerven, T., Wang, L. & Mallants, D. 2010 Geochemical modeling of leaching of Ca, Mg, Al, and Pb from cementitious waste forms. *Cement and Concrete Research* **40** (8), 1298–1305.

Morrow, A. C., Dunstan, R. H. & Coombes, P. J. 2010 Elemental composition at different points of the rainwater harvesting system. *Science of the Total Environment* **408**, 4542–4548.

O'Flaherty, V., Mahony, T., O'Kennedy, R. & Colleran, E. 1998 Effect of pH on growth kinetics and sulphide toxicity thresholds of a range of methanogenic, syntrophic and sulphate-reducing bacteria. *Process Biochemistry* **33** (5), 555–569.

O'Neill, S. W. & Davis, A. P. 2011 Water treatment residual as a bioretention amendment for phosphorus. II: long-term column studies. *Journal of Environmental Engineering* **138** (3), 328–336.

Passeport, E., Hunt, W. F., Line, D. E., Smith, R. A. & Brown, R. A. 2009 Field study of the ability of two grassed bioretention cells to reduce storm-water runoff pollution. *Journal of Irrigation and Drainage Engineering* **135** (4), 505–510.

Piñol, J. & Avila, A. 1992 Streamwater pH, alkalinity, pCO_2 and discharge relationships in some forested Mediterranean catchments. *Journal of Hydrology* **131** (1), 205–225.

R Core Team 2017 *A Language and Environment for Statistical Computing*. R Core Team, R Foundation for Statistical Computing, Vienna, Austria.

Roseen, R. M., Ballestero, T. P., Houle, J. J., Briggs, J. F. & Houle, K. M. 2012 Water quality and hydrologic performance of a porous asphalt pavement as a storm-water treatment strategy in a cold climate. *Journal of Environmental Engineering* **138** (1), 81–89.

Shammas, N. K. 1986 Interactions of temperature, pH, and biomass on the nitrification process. *Journal Water Pollution Control Federation* **58**, 52–59.

Soil Survey Staff 2015 *Web Soil Survey*. Soil Survey Staff, Natural Resources Conservation Service, United States Department of Agriculture. Available: http://websoilsurvey.nrcs.usda.gov/.

Strecker, E. W., Quigley, M. M., Urbonas, B. R., Jones, J. E. & Clary, J. K. 2001 Determining urban storm water BMP effectiveness. *Journal of Water Resources Planning and Management* **127** (3), 144–149.

Sung, M., Kan, C. C., Wan, M. W., Yang, C. R., Wang, J. C., Yu, K. C. & Lee, S. Z. 2010 Rainwater harvesting in schools in Taiwan: system characteristics and water quality. *Water Science and Technology* **61** (7), 1767–1778.

Blue-Green Systems Vol 2 No 1
doi: 10.2166/bgs.2020.914

USEPA 1983 *Methods of Chemical Analysis of Water and Waste*. U.S. Environmental Protection Agency (USEPA), Cincinnati, Ohio. EPA-600/4-79-020.

USEPA 2009 *National Primary Drinking Water Regulations*. U.S. Environmental Protection Agency, Washington, DC. EPA 816-F-09-004. Available: https://www.nrc.gov/docs/ML1307/ML13078A040.pdf.

USEPA 2012 *National Water Quality Criteria – Aquatic Life Criteria Table*. U.S. Environmental Protection Agency (USEPA). https://www.epa.gov/wqc/national-recommended-water-quality-criteria-aquatic-life-criteria-table.

Walsh, C. J., Roy, A. H., Feminella, J. W., Cottingham, P. D., Groffman, P. M. & Morgan, R. P. 2005 The urban stream syndrome: current knowledge and the search for a cure. *Journal of the North American Benthological Society* **24** (3), 706–723.

Wardynski, B. J., Winston, R. J. & Hunt, W. F. 2012 Internal water storage enhances exfiltration and thermal load reduction from permeable pavement in the North Carolina mountains. *Journal of Environmental Engineering* **139** (2), 187–195.

Wilson, C. E., Hunt, W. F., Winston, R. J. & Smith, P. 2014 Assessment of a rainwater harvesting system for pollutant mitigation at a commercial location in Raleigh, NC, USA. *Water Science and Technology: Water Supply* **14** (2), 283–290.

Winston, R. J., Lauffer, M. S., Narayanaswamy, K., McDaniel, A. H., Lipscomb, B. S., Nice, A. J. & Hunt, W. F. 2015 Comparing bridge deck runoff and stormwater control measure quality in North Carolina. *Journal of Environmental Engineering* **141** (1), 04014045.

Winston, R. J., Al-Rubaei, A. M., Blecken, G. T., Viklander, M. & Hunt, W. F. 2016a Maintenance measures for preservation and recovery of permeable pavement surface infiltration rate – the effects of street sweeping, vacuum cleaning, high pressure washing, and milling. *Journal of Environmental Management* **169**, 132–144.

Winston, R. J., Davidson-Bennett, K. M., Buccier, K. M. & Hunt, W. F. 2016b Seasonal variability in stormwater quality treatment of permeable pavements situated over heavy clay and in a cold climate. *Water, Air, & Soil Pollution* **227** (5), 1–21.

Winston, R. J., Dorsey, J. D., Smolek, A. P. & Hunt, W. F. 2018 Hydrologic performance of four permeable pavement systems constructed over low permeability soils in northern Ohio. *Journal of Hydrologic Engineering* **23** (4), 04018007.

Winston, R. J., Arend, K., Dorsey, J. D., Johnson, J. P. & Hunt, W. F. 2020 Hydrologic performance of a permeable pavement and stormwater harvesting treatment train stormwater control measure. *Journal of Sustainable Water in the Built Environment*. **6** (1), 04019011.

Wolock, D. M., Hornberger, G. M., Beven, K. J. & Campbell, W. G. 1989 The relationship of catchment topography and soil hydraulic characteristics to lake alkalinity in the northeastern United States. *Water Resources Research* **25** (5), 829–837.

Xu, W., Fletcher, T., Duncan, H., Bergmann, D., Breman, J. & Burns, M. 2018 Improving the multi-objective performance of rainwater harvesting systems using real-time control technology. *Water* **10** (2), 147.

Zhou, M. & Li, Y. 2001 Phosphorus-sorption characteristics of calcareous soils and limestone from the southern Everglades and adjacent farmlands. *Soil Science Society of America Journal* **65** (5), 1404–1412.

First received 26 April 2019; accepted in revised form 18 December 2019. Available online 3 January 2020